ESC European Society of Cardiology

European Heart Journal - Cardiovascular Imaging (2022) **23**, 1090–1097
https://doi.org/10.1093/ehjci/jeab133

ORIGINAL PAPER

Association between computed tomography-derived tricuspid annular dimensions and prognosis: insights from whole-beat computed tomography assessment

Kensuke Hirasawa[1], Federico Fortuni[1,2], Philippe J. van Rosendael[1], Nina Ajmone Marsan [1], Jeroen J. Bax[1], and Victoria Delgado [1]*

[1]Department of Cardiology, Heart Lung Centre, Leiden University Medical Center, Albinusdreef 2, 2300 RC Leiden, The Netherlands; and [2]Department of Molecular Medicine, Unit of Cardiology, University of Pavia, Pavia, Italy

Received 6 April 2021; editorial decision 20 June 2021; accepted 24 June 2021; online publish-ahead-of-print 19 July 2021

Aims Tricuspid regurgitation (TR) has been associated with outcome in patients treated with transcatheter aortic valve implantation (TAVI). Tricuspid annulus (TA) dimensions are associated with TR. However, the TA is highly dynamic during the cardiac cycle, and the interaction between the TA dimensions, TR, and patient prognosis has never been evaluated. This study aimed to characterize the dynamics of the TA along with the cardiac cycle and its association with prognosis in patients undergoing TAVI.

Methods and results Patients with severe aortic stenosis who underwent whole-beat computed tomography ($n = 393$, mean age 80 ± 7 years, 53% male) were included. The ratio between anterior-posterior (AP) and septal-lateral (SL) diameter of the TA was calculated at end-systole (ES), mid-diastole (MD), and end-diastole (ED) to characterize the TA shape throughout the cardiac cycle. The primary endpoint was all-cause mortality. During a median follow-up of 3.6 (1.7–5.5) years, 146 patients died. While all the TA parameters at ES and MD were not associated with all-cause mortality, a low AP/SL ratio at ED (more circular geometry) was independently related with all-cause mortality (hazard ratio: 4.717, 95% confidence interval: 1.481–15.152; $P = 0.009$). In addition, a more circular TA shape at ED (AP/SL ratio < 1.20) was also associated with more right atrial and ventricular dilation, more frequently significant TR, and a higher prevalence of atrial fibrillation.

Conclusion Circular remodelling of the TA shape at ED is associated with more right atrial and ventricular dilation, and a higher long-term mortality after TAVI. The evaluation of the TA shape at ED may be a useful parameter in the risk stratification of patients undergoing TAVI.

Keywords tricuspid valve • computed tomography • transcatheter aortic valve implantation

Introduction

Tricuspid regurgitation (TR) is a common valvular heart disease in patients with left-sided heart disease and is associated with poor outcomes.[1,2] Dilation of the tricuspid annulus (TA) is the most common cause of secondary TR.[3] Tricuspid valve repair is recommended in patients with significant secondary TR or dilated TA undergoing left-sided heart surgery.[4,5] When using 2D transthoracic echocardiography, the TA diameter should be measured at end-diastole on an apical four-chamber view and TA dilation is defined as a TA diameter

* Corresponding author. Tel: +31 (71) 526 2020; Fax: +31 (71) 526 6809. E-mail: v.delgado@lumc.nl

≥40 mm or >21 mm/m^2.[3] TA dimensions and shape change significantly along with the cardiac cycle and the evidence supporting the assessment of the TA at end-diastole is very limited.[6]

Whole-beat multidetector row computed tomography (MDCT) has a high spatial resolution and represents a powerful imaging modality for assessing 3D cardiac anatomy and dynamics. MDCT is commonly performed in patients with severe aortic stenosis (AS) prior to transcatheter aortic valve implantation (TAVI) to evaluate the optimal prosthesis size and vascular access. AS is frequently associated with TR due to left ventricular (LV) diastolic dysfunction, increased pulmonary pressure, and right ventricular (RV) remodelling.[7–10] Although, MDCT allows the evaluation of the dynamic TA geometry, the association between the various measures of the TA along the cardiac cycle, TR and prognosis in patients undergoing TAVI has not been systematically investigated.

Accordingly, the aim of this study was to characterize the TA geometry changes along the cardiac cycle using MDCT in patients with severe AS and to investigate its association with TR and prognosis after TAVI.

Methods

Patient population

From November 2007 to August 2019, 445 patients with AS underwent whole-beat MDCT prior to TAVI at the Leiden University Medical Center. After excluding patients with cardiac devices ($n = 22$), prior valvular procedures ($n = 5$), insufficient quality of MDCT images ($n = 19$), or those who died within 30 days of the TAVI procedure ($n = 6$), 393 patients were included in this study (Supplementary data online, *Figure*). Baseline clinical data including demographics, cardiovascular risk factors, symptoms, and medications were collected from the medical record system of the cardiology department (EPD vision version 12.5.4; Leiden, The Netherlands). The institutional review board of our institution approved the retrospective analysis of clinically acquired data, and the need for written informed consent was waived. The data that support the findingsof this study are available on reasonable request to the correspondingauthor.

Multi-detector row computed tomography data acquisition and analysis

Clinically indicated MDCT scans were performed for pre-procedural planning of the TAVI procedure using a 64-detector (Aquilion 64, Toshiba Medical Systems, Otawara, Japan) or a 320-detector row computed tomography scanner (Aquilion One, Toshiba Medical Systems, Tochigi-ken, Japan) according to a dedicated cardiac computed tomography protocol, as described in detail before.[11] The median time difference between the date of MDCT and the TAVI procedure was 28 (5–88) days. With a 64-detector row computed tomography scanner, data acquisition was performed gated to the electrocardiogram (ECG) to allow retrospective gating and reconstruction of the data at desired phases of the cardiac cycle (at each 10% of the RR interval). In contrast, with a 320-detector row computed tomography scanner, prospective ECG triggered dose modulation was applied, scanning an entire cardiac cycle and attaining maximal tube current at 75% (when stable heart rate <60 bpm) or 65–85% (when heart rate ≥60 bpm) of the RR interval. Image quality was visually evaluated and the patients were excluded when the images had insufficient contrast opacification of the right heart to delineate the endocardial borders. Reconstructions were acquired at each 10% of the RR interval and these were subsequently transferred to a remote work station enabling offline analysis using dedicated software (3mensio version 10.0, Pie Medical Imaging, Bilthoven, The Netherlands). The whole cardiac cycle was visually analysed to define the reconstructions at the end-systolic (the frame just before TV) and end-diastolic phases (the frame after TV closure). The end-systolic phase was acquired between 30% and 50% of the cardiac cycle and the end-diastolic phase between 80% and 100%.

For volumetric chamber quantification, the endocardial borders of the right and left atria and ventricles were manually traced on every 5-mm slice enabling the calculation of chamber volumes. LV and RV end-diastolic volume (EDV) and end-systolic volume (ESV) were assessed and indexed for body surface area (BSA). Subsequently, LV and RV ejection fraction were calculated using the following formula: EF (%) = [(EDV—ESV)/EDV] × 100. Maximal left atrial and right atrial volumes were measured and were indexed for BSA to calculate the left atrial volume index (LAVI) and the right atrial volume index (RAVI).

For the geometrical analysis of the TA dimensions, an additional package of a specialized software (3mensio Valves workstation, version 10.0, Pie Medical Imaging, Bilthoven, The Netherlands) was used. The TA area, perimeter, antero-posterior (AP), and septal-lateral (SL) diameters were measured at end-systole (the frame just before TV opening), mid-diastole (the middle frame between end-systole and end-diastole), and end-diastole (frame after TV closure) (*Figure 1*). The AP/SL ratio, reflecting the circularity of the TA, was assessed by dividing the AP diameter to the SL diameter.

Transthoracic echocardiography

A comprehensive 2D transthoracic echocardiography was performed within a month prior to TAVI with patients at rest in the left lateral decubitus position using commercially available ultrasound systems equipped with 3.5 MHz or M5S transducers (E9 or E95, GE-Vingmed, Horten, Norway) according to current guidelines.[12,13] All transthoracic echocardiographic images were digitally stored for analysis on an offline workstation (EchoPAC Version 203.0.1, GE Medical Systems, Horten, Norway). Continuous-wave Doppler was used to measure the maximal aortic valve velocities in apical three- or five-chamber views, and the mean gradients were assessed using the modified Bernoulli equation. The aortic valve area was calculated by the continuity equation using the time velocity integrals of the LV outflow tract and the aortic valve and indexed for BSA. The systolic pressure gradient of the RV was quantified with the maximum TR jet velocity according to the modified Bernoulli equation, and subsequently, the estimated right atrial pressure was added to determine the systolic pulmonary artery pressure. The right atrial pressure was estimated from the diameter and respiratory change of the inferior vena cava, as recommended.[12,14] The severity of TR was assessed using an integrated approach as recommended in current guidelines.[15]

Follow-up

The primary endpoint was all-cause mortality after TAVI. Data on mortality were collected by review of the individual medical patient records which are linked to the governmental death registry.

Statistical analysis

Continuous variables are presented as mean ± standard deviation if normally distributed or as median with interquartile range otherwise. Categorical variables were presented as frequencies and percentages. TA dimensions at different timings during the cardiac cycle were compared using the Friedman test. Univariable Cox proportional hazard analysis was performed to investigate the correlates of all-cause mortality after TAVI. Subsequently, multivariable Cox regression analysis was performed

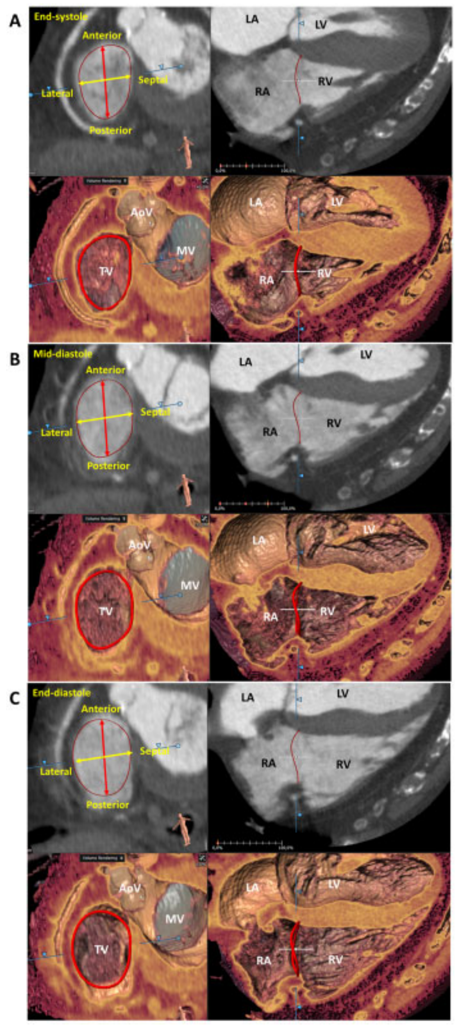

Figure 1 Assessment of tricuspid annular shape using multi-detector row computed tomography. (*A*) end-systole, (*B*) mid-diastole, and (*C*) end-diastole. AoV, aortic valve; LA, left atrium; LV, left ventricle; MV, mitral valve; RA, right atrium; RV, right ventricle; TV, tricuspid valve.

to assess factors that were independently associated with all-cause mortality. Possible confounders with a significant *P* value <0.05 in the univariable analysis were included in the multivariable Cox regression analysis. Hazard ratios (HRs) and the 95% confidence intervals (CIs) were presented. The cut-off value of AP/SL ratio associated with a mortality excess was identified with a spline curve analysis. According to the cut-off value identified for AP/SL ratio, two groups of patients were compared using the χ^2 test for categorical variables, unpaired Student's *t*-test for normally distributed continuous variables, and the Mann–Whitney *U* test for non-normally distributed continuous variables. The Kaplan–Meier analysis and log-rank test were performed to compare the survival of these two groups of patients during the follow-up. A two-sided *P*-value <0.05 was considered statistically significant. The intraclass correlation coefficients (ICCs) were calculated to assess the intra- and inter-observer variability of the TA measurements. Two independent observers (K.H. and P.J.R.) performed TA measurements using MDCT for inter-observer variability analysis. All statistical analysis were performed using SPSS software version 25 (SPSS, Inc., Chicago, IL, USA) and R version 3.4.4 (R Foundation for Statistical Computing, Vienna, Austria).

Results

Overall, 393 patients (53% male), with a mean age of 80 ± 7 years were included in the present analysis. Baseline demographic and echocardiographic parameters are shown in *Table 1*. The majority of the patients had hypertension (77%) and dyslipidaemia (66%). New York Heart Association (NYHA) functional class III–IV heart failure symptoms were observed in 228 patients (58%). Seventy-six patients (19%) had moderate-to-severe TR. Baseline MDCT parameters are shown in *Tables 1 and 2*. The mean LVEF and RVEF were 54 ± 15% and 48 ± 12%, respectively.

While, the overall TA dimensions increased from end-systole to end-diastole, the shape of the TA (AP/SL ratio) remained relatively stable throughout the cardiac cycle (1.23 ± 0.15, 1.22 ± 0.16, and 1.24 ± 0.16, $P = 0.091$).

MDCT associates of all-cause mortality

During a median follow-up of 3.6 (interquartile range 1.7–5.5) years, 146 patients (37%) died. *Table 3* shows the uni- and multivariable Cox regression analyses for all-cause mortality. On the univariable Cox regression analysis, the following parameters showed an association with all-cause mortality: AP/SL ratio at end-diastole, presence of chronic obstructive pulmonary disease, indexed RVESV, RVEF, RAVI, and moderate-to-severe significant TR. While none of the TA dimensions at end-systole and mid-diastole showed an association with all-cause mortality, decrease of the AP/SL ratio at end-diastole (more circular geometry) [HR 4.717 (95% CI: 1.481–15.152), $P = 0.009$] remained independently associated with all-cause mortality after TAVI.

Patients' characteristics according to end-diastolic TA shape and its impact on mortality

The spline curve analysis revealed an excess risk of all-cause mortality for values of the end-diastolic AP/SL ratio <1.20 (*Figure 2*). Accordingly, the patients were classified into two groups: (i) patients with a more elliptic TA shape at end-diastole (AP/SL ratio ≥1.20); and (ii) patients with a more circular TA shape at end-diastole (AP/SL ratio <1.20). Patients with a more circular end-diastolic TA shape (AP/SL ratio <1.20) had higher prevalence of atrial fibrillation and moderate-to-severe TR, larger LAVI, RAVI, and RVEDV and RVESV compared to patients with more elliptical end-diastolic TA shape (AP/SL ratio ≥1.20) (*Table 4*). On Kaplan–Meier survival curve analysis, the 1- and 5-year cumulative survival rates were 89% and 60% for the overall population, 86% and 52% for patients with an AP/SL ratio <1.20, and 92% and 71% for patients with an AP/SL ratio ≥1.20, respectively (*Figure 3*). Patients with an AP/SL ratio <1.20 at end-diastole had higher cumulative rates of all-cause death after TAVI compared to patients with an AP/SL ratio ≥1.20 at end-diastole (χ^2 8.402, log-rank $P = 0.004$).

Table 1 Baseline characteristics of the total population

	n = 393
Age, years	80 ± 7
Male, %	209 (53)
Body surface area, m^2	1.85 ± 0.21
Hypertension, %	301 (77)
Dyslipidaemia, %	259 (66)
Diabetes, %	280 (29)
AF, %	78 (20)
COPD, %	90 (23)
Malignant disease, %	87 (22)
Medication	
ACE inhibitor or ARB, %	214 (55)
Diuretics, %	215 (54)
Beta blockers, %	248 (63)
NYHA classification, %	
I	27 (7%)
II	138 (35%)
III	192 (49%)
IV	36 (9%)
Echocardiographic parameters	
Indexed AVA, cm^2/m^2	0.41 ± 0.11
Mean pressure gradient, mmHg	43 ± 17
Peak TR velocity, m/s	2.6 ± 0.6
SPAP, mmHg	36 ± 13
TAPSE, mm	18 ± 4
TA diameter, mm	34 ± 5
TR grade ≥3, %	76 (19)
MDCT parameters	
Indexed LVEDV, mL/m^2	87 ± 26
Indexed LVESV, mL/m^2	43 ± 26
LVEF, %	54 ± 15
LAVI, mL/m^2	62 ± 19
Indexed RVEDV, mL/m^2	79 ± 20
Indexed RVESV, mL/m^2	41 ± 16
RVEF, %	48 ± 12
RAVI, mL/m^2	60 ± 23

Values are expressed as mean ± SD or *n* (%).
ACE, angiotensin-converting enzyme; AF, atrial fibrillation; ARB, angiotensin receptor blocker; AVA, aortic valve area; COPD, chronic obstructive pulmonary disease; LAVI, left atrial volume index; LVEDV, left ventricular end-diastolic volume; LVEF, left ventricular ejection fraction; LVESV, left ventricular end-systole volume; NYHA, New York Heart Association; RAVI, right atrial volume index; RVEDV, right ventricular end-diastolic volume; RVEF, right ventricular ejection fraction; RVESV, right ventricular end-systolic volume; SPAP, systolic pulmonary artery pressure; TA, tricuspid annulus; TAVI, transcatheter aortic valve implantation; TAPSE, tricuspid annular plane systolic excursion; TR, tricuspid regurgitation.

Reproducibility

The ICCs for the TA measurements were calculated in 40 randomly selected patients at each cardiac phase for the reproducibility analysis. For the intra-observer variability, the ICCs for TA area, perimeter, and AP/SL ratio were 0.922, 0.927, and 0.836 at end-systole; 0.940, 0.940, and 0.827 at mid-diastole; and 0.950, 0.941, and 0.926 at end-diastole. For the inter-observer variability, the ICCs for TA area, perimeter, and AP/SL ratio were 0.888, 0.872, and 0.820 at end-systole; 0.918, 0.890, and 0.820 at mid-diastole; and 0.944, 0.884, and 0.862 at end-diastole.

Discussion

The main findings of this study can be summarized as follows: (i) in patients with severe AS, TA shape measured with MDCT did not change along the cardiac cycle, (ii) the end-diastolic AP/SL ratio, reflecting the circularity of TA, was the only TA parameter associated with long-term mortality after TAVI, whereas other TA dimensions and shape indices at end-systole and mid-diastole were not, and (iii) patients with circular end-diastolic TA shape had larger RA and RV, higher prevalence of AF and significant TR compared to those with higher end-diastolic AP/SL ratio (≥1.20).

TA geometry across the cardiac cycle in patients with severe AS

Current guidelines recommend measuring the TA diameter at end-diastole to evaluate the indication for tricuspid valve surgery at the time of left-sided heart surgery.[3–5] However, it is not clear which imaging modality should be used to assess the TA dimensions. The most frequently used imaging technique for TA assessment is 2D transthoracic echocardiography, which can only identify the SL diameter of the TA and does not provide any information on TA shape.[16] Left-sided valvular heart disease can induce RV remodelling, secondary TR, and asymmetric TA dilatation that cannot be derived from a 2D imaging technique. Moreover, TA size and shape vary throughout the cardiac cycle and the evidence to support the assessment of the TA at end-diastole is limited. Addetia *et al.*[6] demonstrated that the TA size measured with 3D transthoracic echocardiography may change ∼30% between systole and diastole.

In contrast to other imaging modalities, whole-beat MDCT provides high resolution data that allow the assessment of 3D geometry and dynamics of the TA and the measurement of AP and SL diameters. The AP and SL diameters of TA can be integrated into a ratio (i.e. AP/SL ratio) to characterize the TA shape. In this study, TA measurements and dynamics were characterized along the cardiac cycle in patients with severe AS using MDCT. As shown in previous literature,[6,17] the overall TA size was highly variable in the different cardiac phases and increased from end-systole to end-diastole, whereas the TA shape was consistent throughout the cardiac cycle.

Ton-Nu *et al.*[18] demonstrated that patients with significant secondary TR had larger, more planar, and circular geometry of TA compared to controls using 3D echocardiography. A recent publication also showed the circular TA shape using 3D transoesophageal echocardiography in patients with secondary TR and atrial fibrillation.[19] These influences of significant TR and atrial fibrillation on TA shape were similarly observed in the present cohort of TAVI patients. Using MDCT, this study confirms the abovementioned findings with a more accurate imaging technique and adds data on the relation of TA shape with TR and with prognosis independently of TR in patients with AS.

Table 2 TA measurements using multidetector computed tomography

n = 393	End-systole	Mid-diastole	End-diastole	*P* value
Indexed TA area, cm^2/m^2	5.5 ± 1.3	6.1 ± 1.2	6.8 ± 1.5	<0.001
Indexed TA perimeter, mm/m^2	63 ± 8	66 ± 8	71 ± 10	<0.001
Indexed AP diameter, mm/m^2	22 ± 3	23 ± 3	24 ± 3	<0.001
Indexed SL diameter, mm/m^2	18 ± 3	19 ± 3	20 ± 3	<0.001
AP/SL ratio	1.23 ± 0.15	1.22 ± 0.16	1.24 ± 0.16	0.091

Values are expressed as mean ± SD or *n* (%).
AP, anterior-posterior; SL, septal-lateral; TA, tricuspid annulus.

Table 3 Univariate and multivariate Cox regression analysis for all-cause mortality

	Univariate		Multivariate	
	HR (95% CI)	*P*	HR (95% CI)	*P*
End-diastole				
Indexed TA area, per 1 cm^2/m^2 increase	1.080 (0.969–1.204)	0.164		
Indexed AP diameter, per 1 mm/m^2 increase	0.972 (0.916–1.031)	0.347		
Indexed SL diameter, per 1 mm/m^2 increase	1.027 (0.982–1.073)	0.251		
AP/SL ratio, per 1 unit decrease	6.536 (2.088–20.408)	0.001	4.717 (1.481–15.152)	0.009
Mid-diastole				
Indexed TA area, per 1 cm^2/m^2 increase	1.086 (0.957–1.231)	0.201		
Indexed AP diameter, per 1 mm/m^2 increase	1.007 (0.948–1.070)	0.826		
Indexed SL diameter, per 1 mm/m^2 increase	1.040 (0.982–1.102)	0.182		
AP/SL ratio, per 1 unit decrease	2.208 (0.722–6.757)	0.165		
End-systole				
Indexed TA area, per 1 cm^2/m^2 increase	1.089 (0.952–1.246)	0.214		
Indexed AP diameter, per 1 mm/m^2 increase	1.009 (0.950–1.072)	0.771		
Indexed SL diameter, per 1 mm/m^2 increase	1.017 (0.959–1.078)	0.572		
AP/SL ratio, per 1 unit decrease	1.250 (0.431–3.623)	0.681		
Age, per 1 years increase	0.981 (0.961–1.002)	0.079		
Male, yes/no	1.263 (0.913–1.747)	0.159		
COPD, yes/no	1.733 (1.221–2.460)	0.002	1.972 (1.381–2.817)	<0.001
Malignant disease, yes/no	1.153 (0.795–1.672)	0.454		
Indexed RVEDV, per 1 mL/m^2 increase	1.003 (0.995–1.011)	0.551		
Indexed RVESV, per 1 mL/m^2 increase	1.013 (1.004–1.022)	0.006		
RVEF, per 1% increase	0.975 (0.962–0.989)	<0.001	0.978 (0.964–0.992)	0.002
LAVI, per 1 mL/m^2 increase	1.006 (0.999–1.014)	0.085		
RAVI, per 1 mL/m^2 increase	1.012 (1.006–1.019)	<0.001		
Indexed LVEDV, per 1 mL/m^2 increase	0.999 (0.992–1.005)	0.659		
Indexed LVESV, per 1 mL/m^2 increase	1.001 (0.995–1.007)	0.683		
LVEF, per 1% increase	0.995 (0.985–1.005)	0.349		
SPAP, per 1 mmHg increase	1.005 (0.993–1.018)	0.418		
TAPSE, per 1 mm increase	0.989 (0.951–1.029)	0.596		
TA diameter measured by TTE, per 1 mm increase	1.027 (0.997–1.059)	0.077		
TR grade ≥3, yes/no	1.718 (1.192–2.476)	0.004	1.438 (0.968–2.137)	0.072
AF, yes/no	1.305 (0.890–1.914)	0.173		

AF, atrial fibrillation; AP, anterior-posterior; CI, confidence interval; COPD, chronic obstructive pulmonary disease; HR, hazard ratio; LAVI, left atrial volume index; LVEDV, left ventricular end-diastolic volume; LVEF, left ventricular ejection fraction; LVESV, left ventricular end-systolic volume; RAVI, right atrial volume index; RVEDV, right ventricular end-diastolic volume; RVEF, right ventricular ejection fraction; RVESV, right ventricular end-systolic volume; SPAP, systolic pulmonary artery pressure; TA, tricuspid annulus; TAPSE, tricuspid annular plane systolic excursion; TAVI, transcatheter aortic valve implantation; TR, tricuspid regurgitation; TTE, transthoracic echocardiography.

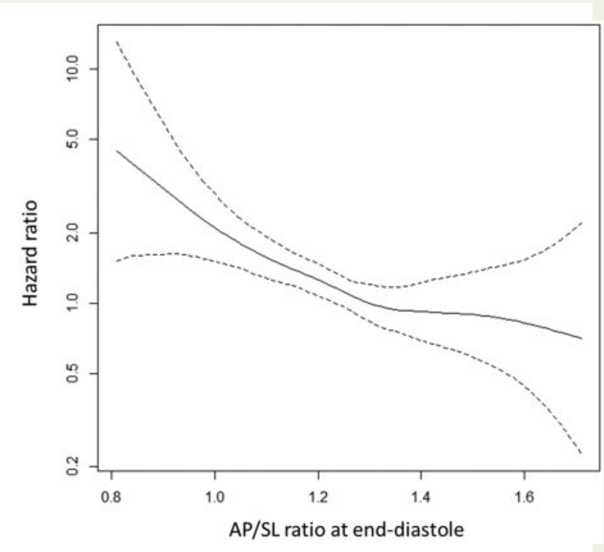

Figure 2 Spline curve analysis for AP/SL ratio at end-diastole vs. all-cause mortality. AP, antero-posterior; SL, septal-lateral.

Prognostic and clinical implications

In the present cohort, while none of the conventional TA dimensional parameters were associated with prognosis, the shape of the TA (AP/SL ratio) at end-diastole was independently associated with all-cause mortality. For patients with secondary TR, concomitant tricuspid valve repair has been recommended in patients with severe TR and/or increased TA diameter (≥40 mm or ≥21 mm/m^2) at the time of left-sided heart surgery.[4,5] These recommendations are based on several observational studies including patients who underwent mitral valve surgery.[2,20,21] Although severe AS is also frequently associated with significant TR, the utility of TA shape and dimensions for risk stratification and to evaluate the indication for tricuspid valve repair has never been tested.

A previous study showed that a TA diameter ≥37 mm was associated with persistent TR after TAVI.[22] However, no study has shown the association between TA dimensions and outcomes after TAVI. The preprocedural evaluation of patients referred for TAVI frequently includes a whole-beat MDCT which enables a 3D characterization of the TA geometry. Severe TR is common in patients with severe AS undergoing TAVI and has been shown to impact negatively on the survival of those patients. In addition, MDCT is

Table 4 Patients characteristics according to AP/SL ratio at end-diastole

	AP/SL ratio at end-diastole ≥1.20 (n = 167)	AP/SL ratio at end-diastole <1.20 (n = 226)	P value
Age, years	79 ± 8	80 ± 7	0.123
Male, %	98 (59)	111 (49)	0.060
Body surface area, m^2	1.87 ± 0.20	1.84 ± 0.21	0.265
AF, %	14 (8)	64 (28)	<0.001
NYHA classification, %			
I	13 (8)	14 (6)	0.714
II	54 (32)	84 (37)	
III	83 (50)	109 (48)	
IV	17 (10)	19 (8)	
Echocardiographic parameters			
Indexed AVA, cm^2/m^2	0.42 ± 0.11	0.40 ± 0.11	0.062
Mean pressure gradient, mmHg	42 ± 16	44 ± 18	0.335
SPAP, mmHg	34 ± 12	37 ± 14	0.117
TAPSE, mm	18 ± 4	18 ± 4	0.420
TR grade ≥3, %	18 (11)	58 (26)	<0.001
MDCT parameters			
Indexed LVEDV, mL/m^2	90 ± 28	85 ± 24	0.069
Indexed LVESV, mL/m^2	44 ± 29	41 ± 24	0.235
LVEF, %	54 ± 16	54 ± 15	0.914
LAVI, mL/m^2	57 ± 13	66 ± 22	<0.001
Indexed RVEDV, mL/m^2	73 ± 16	83 ± 21	<0.001
Indexed RVESV, mL/m^2	37 ± 13	44 ± 17	<0.001
RVEF, %	50 ± 11	47 ± 12	0.051
RAVI, mL/m^2	50 ± 15	68 ± 24	<0.001

Values are expressed as mean ± SD or n (%).
AF, atrial fibrillation; AVA, aortic valve area; NYHA, New York Heart Association; PAP, pulmonary artery pressure; TA, tricuspid annulus; TAVI, transcatheter aortic valve implantation; SPAP, systolic pulmonary artery pressure; TAPSE, tricuspid annular plane systolic excursion; TR, tricuspid regurgitation.

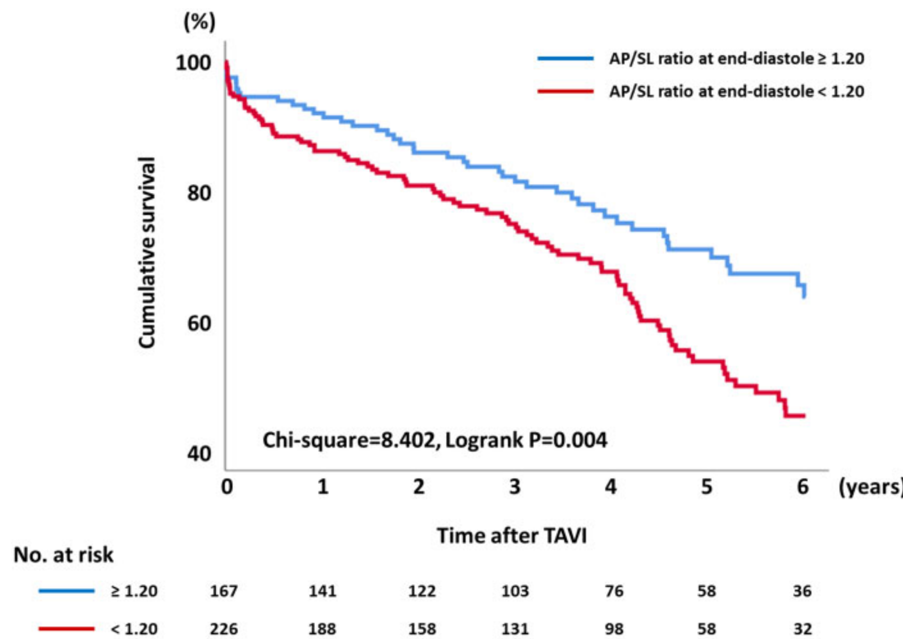

Figure 3 Kaplan–Meier analysis for all-cause mortality after TAVI according to AP/SL ratio at end-diastole. AP, antero-posterior; SL, septal-lateral; TAVI, transcatheter aortic valve implantation.

also frequently used for the evaluation of other transcatheter interventions for structural heart disease. Minor adaptations to the MDCT protocol to ensure adequate right heart visualization, could be implemented to enable TA assessment in patients who undergo MDCT prior to a transcatheter intervention for structural heart disease. The current study demonstrates that a more circular TA shape at end-diastole is the only TA parameter associated with prognosis in patients undergoing TAVI. TA dimensions during systole could be influenced by several factors including the systolic pulmonary pressure and/or RV systolic function. In contrast, the end-diastolic TA dimensions are mainly influenced by RV volume and may reflect the degree of TA remodelling more directly as compared to the other cardiac phases. Therefore, we speculate that particularly the end-diastolic TA shape is associated with the occurrence of post-procedural TR and mortality.

This finding provides further evidence on the importance of assessing TA at end-diastole and suggests that the end-diastolic TA shape may have a crucial role for the selection of patients with severe AS who can benefit also from transcatheter therapies on the tricuspid valve (since the patient population of the present study entailed patients undergoing TAVI).[23] Although we demonstrated that a more circular TA is associated with poor outcomes, further dedicated studies would be needed to examine the utility of concomitant tricuspid valve repair according to TA shape in selected patients undergoing TAVI.

Limitations

First, the current retrospective observational study has limitations inherent to the nature of its study design. Second, the inclusion limited to patients with good contrast-enhanced MDCT image quality may represent a source of selection bias. Thus, patients with high heart rate, uncontrolled arrhythmia, and severe renal dysfunction may have been excluded. Furthermore, a significant number of patients ($n = 555$) were excluded because of lack of a whole-beat MDCT data which may incur in a selection bias. The main reasons for the lack of whole-beat MDCT data were that the referral centres only perform the MDCT acquisition at 75% of the RR interval and the presence of renal dysfunction and poor clinical condition that would increase the risk of acute kidney injury which has a detrimental effect on TAVI outcomes. When MDCT data were not available, a 3D transoesophageal echocardiography was performed to size the aortic annulus. Third, survival data were obtained from governmental registry which does not include the reason of death. Thus, we could not assess whether the patients died from a cardiac or non-cardiac cause. Finally, the reconstruction of every 10% RR intervals of the cardiac cycle may not provide sufficient temporal resolution to characterize the dynamics of the TA.

Conclusion

End-diastolic TA shape is the only TA dimensional index associated with prognosis in patients with severe AS undergoing TAVI. These results support the evaluation of TA shape at end-diastole which may improve the risk stratification of patients with severe AS.

Supplementary data

Supplementary data are available at *European Heart Journal - Cardiovascular Imaging* online.

Funding

K.H. was financially supported by an ESC research grant. The reference of application number is R-2018-18122.

Conflict of interest: Department of Cardiology of the Leiden University Medical Center received research grants from Abbott Vascular, Bioventrix, Medtronic, Biotronik, Boston Scientific, GE Healthcare, and Edwards Lifesciences. J.B. and N.A.M. received speaking fees from Abbott Vascular. V.D. received speaker fees from Abbott Vascular, Medtronic, MSD, Edwards Lifesciences, and GE Healthcare. The remaining authors have no conflict of interest to declare.

References

1. Song H, Kim MJ, Chung CH, Choo SJ, Song MG, Song JM *et al.* Factors associated with development of late significant tricuspid regurgitation after successful left-sided valve surgery. *Heart* 2009;**95**:931–6.
2. Dreyfus GD, Corbi PJ, Chan KM, Bahrami T. Secondary tricuspid regurgitation or dilatation: which should be the criteria for surgical repair? *Ann Thorac Surg* 2005;**79**:127–32.
3. Zoghbi WA, Adams D, Bonow RO, Enriquez-Sarano M, Foster E, Grayburn PA *et al.* Recommendations for noninvasive evaluation of native valvular regurgitation: a report from the American Society of Echocardiography developed in collaboration with the Society for Cardiovascular Magnetic Resonance. *J Am Soc Echocardiogr* 2017;**30**:303–71.
4. Baumgartner H, Falk V, Bax JJ, De Bonis M, Hamm C, Holm PJ *et al.*; ESC Scientific Document Group. 2017 ESC/EACTS guidelines for the management of valvular heart disease. *Eur Heart J* 2017;**38**:2739–91.
5. Nishimura RA, Otto CM, Bonow RO, Carabello BA, Erwin JP 3rd, Guyton RA *et al.*; American College of Cardiology/American Heart Association Task Force on Practice Guidelines. 2014 AHA/ACC guideline for the management of patients with valvular heart disease: executive summary: a report of the American College of Cardiology/American Heart Association task force on practice guidelines. *J Am Coll Cardiol* 2014;**63**:2438–88.
6. Addetia K, Muraru D, Veronesi F, Jenei C, Cavalli G, Besser SA *et al.* 3-dimensional echocardiographic analysis of the tricuspid annulus provides new insights into tricuspid valve geometry and dynamics. *JACC Cardiovasc Imaging* 2019;**12**:401–12.
7. Lindman BR, Maniar HS, Jaber WA, Lerakis S, Mack MJ, Suri RM *et al.* Effect of tricuspid regurgitation and the right heart on survival after transcatheter aortic valve replacement: insights from the placement of aortic transcatheter valves ii inoperable cohort. *Circ Cardiovasc Interv* 2015;**8**.
8. Schwartz LA, Rozenbaum Z, Ghantous E, Kramarz J, Biner S, Ghermezi M *et al.* Impact of right ventricular dysfunction and tricuspid regurgitation on outcomes in patients undergoing transcatheter aortic valve replacement. *J Am Soc Echocardiogr* 2017;**30**:36–46.
9. Tastet L, Tribouilloy C, Marechaux S, Vollema EM, Delgado V, Salaun E *et al.* Staging cardiac damage in patients with asymptomatic aortic valve stenosis. *J Am Coll Cardiol* 2019;**74**:550–63.
10. Vollema EM, Amanullah MR, Ng ACT, van der Bijl P, Prevedello F, Sin YK *et al.* Staging cardiac damage in patients with symptomatic aortic valve stenosis. *J Am Coll Cardiol* 2019;**74**:538–49.
11. van Rosendael PJ, Joyce E, Katsanos S, Debonnaire P, Kamperidis V, van der Kley F *et al.* Tricuspid valve remodelling in functional tricuspid regurgitation: multidetector row computed tomography insights. *Eur Heart J Cardiovasc Imaging* 2016;**17**:96–105.
12. Lancellotti P, Tribouilloy C, Hagendorff A, Popescu BA, Edvardsen T, Pierard LA *et al.*; Scientific Document Committee of the European Association of Cardiovascular Imaging. Recommendations for the echocardiographic assessment of native valvular regurgitation: an executive summary from the European Association of Cardiovascular Imaging. *Eur Heart J Cardiovasc Imaging* 2013;**14**:611–44.
13. Lang RM, Badano LP, Mor-Avi V, Afilalo J, Armstrong A, Ernande L *et al.* Recommendations for cardiac chamber quantification by echocardiography in adults: an update from the American Society of Echocardiography and the European Association of Cardiovascular Imaging. *J Am Soc Echocardiogr* 2015;**28**:1–39.e14.
14. Rudski LG, Lai WW, Afilalo J, Hua L, Handschumacher MD, Chandrasekaran K *et al.* Guidelines for the echocardiographic assessment of the right heart in adults: a report from the American Society of Echocardiography endorsed by the European Association of Echocardiography, a registered branch of the European Society of Cardiology, and the Canadian Society of Echocardiography. *J Am Soc Echocardiogr* 2010;**23**:685–713; quiz 786–8.
15. Topilsky Y, Maltais S, Medina Inojosa J, Oguz D, Michelena H, Maalouf J *et al.* Burden of tricuspid regurgitation in patients diagnosed in the community setting. *JACC Cardiovasc Imaging* 2019;**12**:433–42.
16. Badano LP, Hahn R, Rodriguez-Zanella H, Araiza Garaygordobil D, Ochoa-Jimenez RC, Muraru D. Morphological assessment of the tricuspid apparatus and grading regurgitation severity in patients with functional tricuspid regurgitation: thinking outside the box. *JACC Cardiovasc Imaging* 2019;**12**:652–64.
17. Fukuda S, Saracino G, Matsumura Y, Daimon M, Tran H, Greenberg NL *et al.* Three-dimensional geometry of the tricuspid annulus in healthy subjects and in patients with functional tricuspid regurgitation: a real-time, 3-dimensional echocardiographic study. *Circulation* 2006;**114**:I-492–8.
18. Ton-Nu TT, Levine RA, Handschumacher MD, Dorer DJ, Yosefy C, Fan D *et al.* Geometric determinants of functional tricuspid regurgitation: insights from 3-dimensional echocardiography. *Circulation* 2006;**114**:143–9.
19. Utsunomiya H, Itabashi Y, Kobayashi S, Rader F, Siegel RJ, Shiota T. Clinical impact of size, shape, and orientation of the tricuspid annulus in tricuspid regurgitation as assessed by three-dimensional echocardiography. *J Am Soc Echocardiogr* 2020;**33**:191–200.e191.
20. Colombo T, Russo C, Ciliberto GR, Lanfranconi M, Bruschi G, Agati S *et al.* Tricuspid regurgitation secondary to mitral valve disease: tricuspid annulus function as guide to tricuspid valve repair. *Cardiovasc Surg* 2001;**9**:369–77.
21. Van de Veire NR, Braun J, Delgado V, Versteegh MI, Dion RA, Klautz RJ *et al.* Tricuspid annuloplasty prevents right ventricular dilatation and progression of tricuspid regurgitation in patients with tricuspid annular dilatation undergoing mitral valve repair. *J Thorac Cardiovasc Surg* 2011;**141**:1431–9.
22. Yoshida J, Ikenaga H, Hayashi A, Yamaguchi S, Nagaura T, Rader F *et al.* Predictors and outcomes of persistent tricuspid regurgitation after transcatheter aortic valve implantation. *Am J Cardiol* 2019;**124**:772–80.
23. Nickenig G, Weber M, Schueler R, Hausleiter J, Nabauer M, von Bardeleben RS *et al.* 6-month outcomes of tricuspid valve reconstruction for patients with severe tricuspid regurgitation. *J Am Coll Cardiol* 2019;**73**:1905–15.